JOURNAL OF APPLIED POLYMER SCIENCE VOL. 20, 1077–1093 (1976)

Morphology Development During Shearing of Poly(ethylene Oxide) Melts

ROBERT D. ULRICH* and FRASER P. PRICE, *Polymer Science and Engineering, University of Massachusetts, Amherst, Massachusetts 01002*

Synopsis

A parallel glass-plate rotary shearing device has been constructed. This device allows direct observation of the crystallization of polymeric melts being subjected to a constant rate of shear under controlled temperature conditions. Polarized light microscopy and small-angle light-scattering techniques were employed to study the kinetics and morphology of poly(ethylene oxide) melts as they crystallized under various combinations of supercooling and shear rate. The techniques of epimicroscopy, differential scanning calorimetry, and wide-angle x-ray diffraction were used to study the already crystallized material. Crystalline aggregates developing from sheared melts showed a sheaf-like lamellar morphology. The long axes of the sheaf-like structures oriented perpendicular to the flow direction when crystallized under shear. This behavior can be explained in terms of hydrodynamic theory.

INTRODUCTION

The majority of research dealing with stress-crystallized materials has been carried out with elastomers or crosslinked systems. It appears that as elongation during crystallization is increased, the morphology changes from spherical to aciform, to extended chain.[1,2] This is confirmed by kinetic studies that indicate the growth habit changing from three dimensions to one dimension with increasing elongation. These studies also indicate that nucleation rate becomes relatively more important than growth rate as extension is increased.[3] The critical point is brought out that molecular orientation rather than macrodeformation is the controlling factor in these results.[4]

If dilute polymer solutions are stirred during crystallization, a fibrous "shish-kebab" structure is produced.[5–8] It has been found that a critical extensional flow rate,[9] or a stirrer speed[10] at which Taylor vortices are formed, is necessary for the production of this morphology. The general crystallization mechanism seems to be production of an extended chain backbone which acts as a nucleus for epitaxial growth of the lamellar kebabs.[11–14]

Between the extremes of dilute solutions and elastomers is the area of melts. Studies have shown that stressed melts will crystallize with kinetics and morphologies different from those for the quiescent case and rather similar to those seen for stress-crystallized elastomers.[15–23]

Unfortunately, most kinetic and morphological studies have been carried out after the fact or in a nonquantitative manner. However, Haas and Max-

* Present address: Monsanto Textiles Co., P.O. Box 12830, Pensacola, Fla. 32575

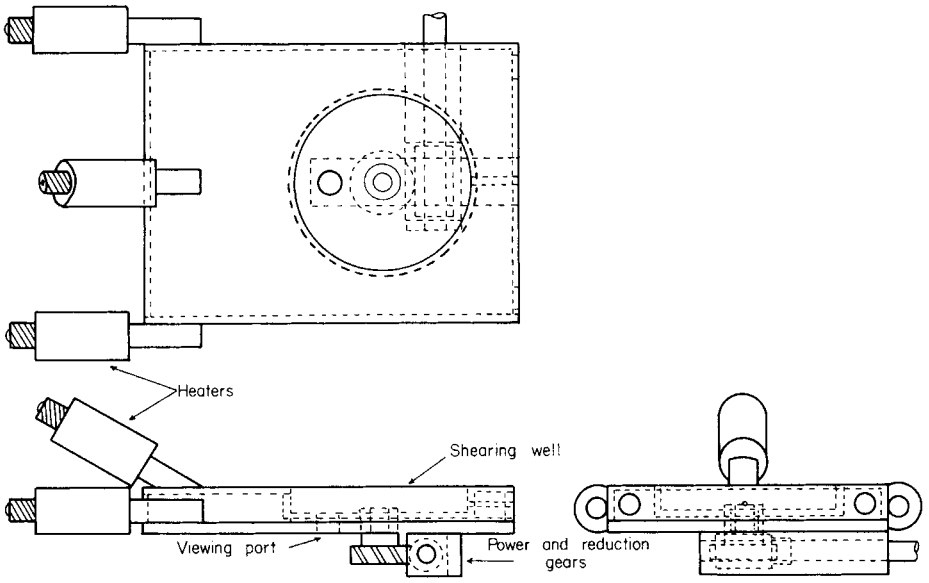

Fig. 1. Shearing device.

well[24] have studied the morphology of thin films of polyethylene and polybutene-1 during crystallization under constant shear stress.

The purpose of the research reported here was to study the morphology of a polymer crystallizing under defined shear and temperature conditions in a relatively thick specimen such that artificial boundary conditions were not imposed on the sample.

INSTRUMENTATION

In order to fulfill the purpose of this research, it was necessary to construct an instrument that would allow microscopic observation of a polymer crystallizing in a defined shear field under controlled temperature conditions. Additionally, the polymer sample had to be thick enough to allow three-dimensional development of morphology.

The device constructed for these studies is shown in Figures 1 and 2. It consists of a hollow brass block that surrounds a shearing well 1⅞ in. in diameter by ¼ in. deep. A bottom glass plate on the shearing well is stationary while the top glass plate rotates. Heaters on the block serve to melt the polymer sample, which can then be quickly cooled to the desired crystallization temperature by circulation of a fluid through the brass block from a constant-temperature bath. The temperature of the polymer is monitored by a fine thermocouple that passes through the side of the shearing wall. A viewing port on the bottom of the brass block allows the shearing device to replace the stage of an optical microscope or be used in small-angle light-scattering studies.

To the bottom of the brass block are attached the power transmission and speed reduction gears that are driven by a constant-speed motor and in turn drive the top glass shearing plate.

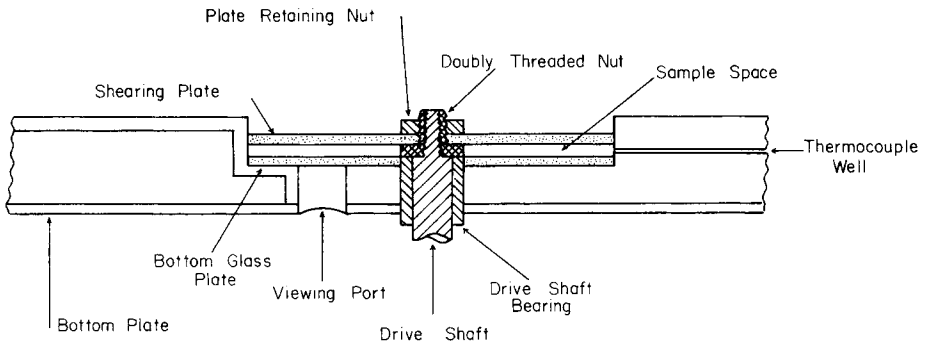

Fig. 2. Detail of shearing well.

The fact that the instrument is a parallel-plate shearing device dictates a radially inhomogeneous shear field. However, one is observing a small annulus of the shear field across which there is relatively small variation. It is additionally observed that particles exhibit little or no radial migration within the field of view. Hence, the observed shear field is essentially homogeneous. A simple Newtonian relationship of $\dot{\gamma} = v/x$ is taken as a first approximation, where $\dot{\gamma}$ is the shear rate, v the plate velocity, and x the plate separation. All experiments reported here were conducted with x at 0.049 ± 0.001 in.

MATERIALS STUDIED

Poly(ethylene oxide) (PEO) was chosen as the material to be studied for the following reasons: (1) convenient melting and crystallization temperature range; (2) forms large aggregates of crystallites; (3) relatively low nucleation density; (4) previous experience with kinetics and morphology of PEO crystallization[25–33]; (5) known to produce highly oriented crystals; and (6) available in range of molecular weights that exhibit orientational effects.

Samples of poly(ethylene oxide) marketed under the tradenames Carbowax 20-M and WSR-205 were kindly supplied by Dr. F. E. Bailey of Union Carbide Corp.

Analysis of the Carbowax 20-M indicated an ash level of 0.96% by weight, most probably due to catalyst residue. GPC analysis indicated a $\bar{M}_w$ of 395,000 and $\bar{M}_n$ of 26,600. WSR-205 yielded a $\bar{M}_w$ of 506,000 and $\bar{M}_n$ of 38,300. The high value of $\bar{M}_w$ for the Carbowax 20-M was due to a high molecular weight tail. Samples were run in m-cresol at 100°C by DeBell and Richardson, Inc., of Enfield, Connecticut.

The Carbowax 20-M sample was studied in its as-received state, while the WSR-205 was mixed with the 20-M to a 4.7% level by a dilution and freeze-drying technique.

Rheological characterization of the samples carried out in a Weissenberg rheogoniometer indicated Newtonian behavior in the range of temperatures and shear rates studied.

Melting point characterization on a Perkin-Elmer DSC-1B was carried out at 2.5°C/min and yielded a value of 64.5 ± 0.5°C for the Carbowax 20-M sample.

EXPERIMENTAL

Utilization of the previously described shearing device is identical for all methods of data collection. The device is securely mounted on whatever piece of equipment is being used for data collection. With the top shearing plate removed, solid polymer is introduced into the shearing well and the heaters turned on. After the polymer has melted, and all air bubbles have been released, the top shearing plate is placed in position. This procedure need be repeated between each crystallization run only if air bubbles are introduced during the previous run or the shearing plate cracks due to the stress generated in shearing the semimolten polymer.

Each crystallization run begins by heating the material in the shearing well to a temperature for a period of time sufficient to remove any predetermined nuclei. For the Carbowax 20-M, this was 100°C for 15 min.[32,33] After this time, the desired speed is set and shearing begun.

The melt heaters are then turned off and the cooling liquid (already at the desired crystallization temperature) introduced into the shearing device. Introduction of the cooling liquid is taken as a nominal time zero. Data collection begins at an appropriate time during the crystallization process and is carried out until a point is reached at which the shearing plate may crack due to the stress or crystallization is complete.

Photographic measurements are carried out with the shearing device mounted on the stage of a Zeiss Standard RA light microscope equipped with a polarizer and analyzer. The light source is a Zeiss-Ukatron-60 high-speed flash. Under the conditions studied, movement of the particles being observed within the duration of the flash is less than the resolution of the optical system. The technique consists of taking photographs at predetermined time intervals during the crystallization process and then enlarging them such that they may be analyzed for the number, sizes, and orientations of the crystalline entities visible within the field. This technique provides a large amount of information but is also extremely tedious.

The experiments are carried out several times with the microscope focused at different depths within the sample. Crystallization experiments at shear rates of 0, 8, 12, and 22 sec^{-1} have been conducted at temperatures of 50.4°, 51.6°, and 53.8°C.

A light-scattering device utilizing a HeNe laser described by Stein and Erhardt[34] has been utilized to follow the crystallization of the polymer melt in both the sheared and quiescent cases. Patterns of the H_v and V_v types are recorded on photographic film at predetermined time intervals as crystallization develops. The photographs are then analyzed with a microdensitometer or utilized for qualitative information.

Characterization of already crystallized samples is carried out using epimicroscopy, transmission electron microscopy, wide-angle x-ray, and differential scanning calorimetry.

RESULTS

As already stated, the crystallization of the polymers under both shear and quiescent conditions is photographed as it occurs. The initial morphology of

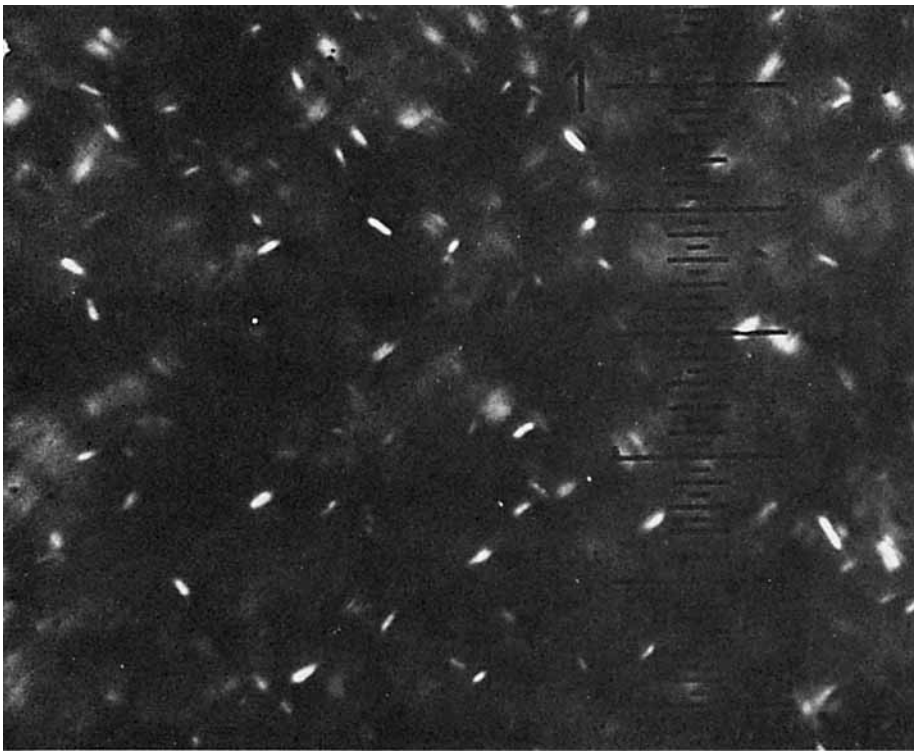

Fig. 3. Photomicrograph of developing rod-like crystalline aggregates under quiescent conditions in Carbowax 20-M. Crossed polars; 17.5 μ per scale division.

the growing crystallites is in the form of a prolate ellipsoid. For quiescent conditions, the orientation of these ellipsoids is random through the melt, as can be seen in Figure 3. As the shear rate is increased, the preferred orientation of the semimajor axis becomes 90° to shear direction. This is shown in Figure 4. The distribution of angles is measured to the nearest five degrees. The fractional frequencies of occurrence of each angle to the shear direction for 0, 8, 12, and 22 sec^{-1} at each temperature were recorded. The results for crystallization at 51.6°C are shown in Figure 5. As the temperature is decreased, or the viscosity increased through addition of high molecular weight material, the distribution for each of the sheared cases shifts to the high angles. It has been demonstrated that these effects are not artifacts of the optical system employed.

No anisotropy of the rod-like entities could be determined by polarized light microscopy. Also, no Maltese cross pattern indicative of spherulitic growth could be seen in the crystalline entities. Hence, the term crystalline aggregates will be used.

A further observation is that the crystalline aggregates appear to break up during shear. This is possibly confirmed by kinetic data that will be discussed in another paper, as well as the results of Fritzsche.[35]

Small-angle light-scattering patterns were photographed during the crystallization of the PEO in the shearing instrument. All quiescent and shear experiments were carried out at 53.6°C. All shear experiments were carried

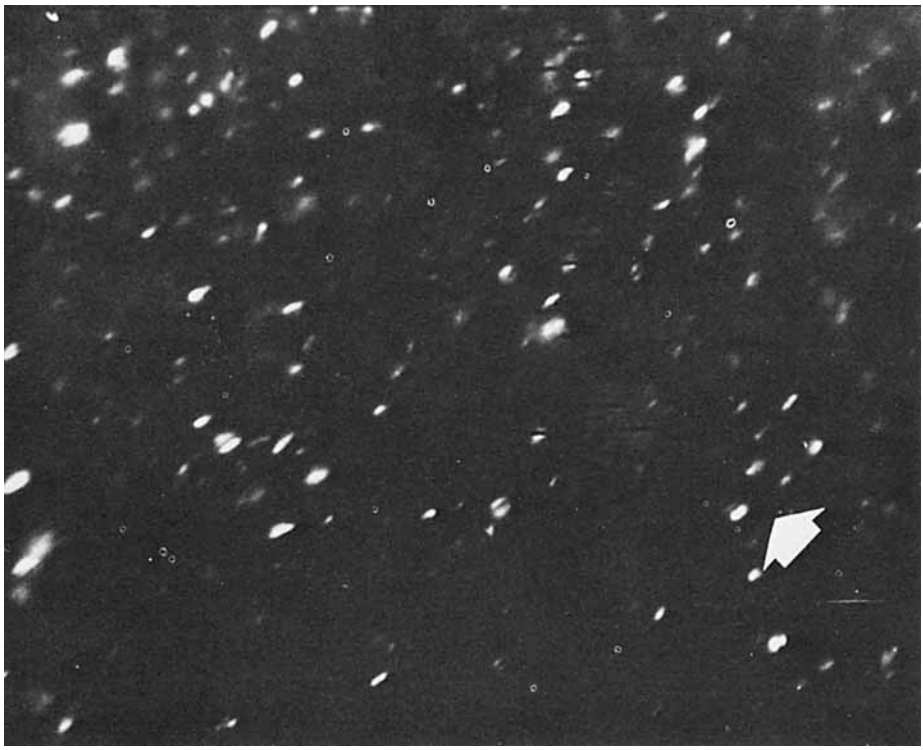

Fig. 4. Photomicrograph of developing rod-like crystalline aggregates and their orientation normal to the shear or flow direction (arrow) in Carbowax 20-M. Same magnification as Fig. 3.

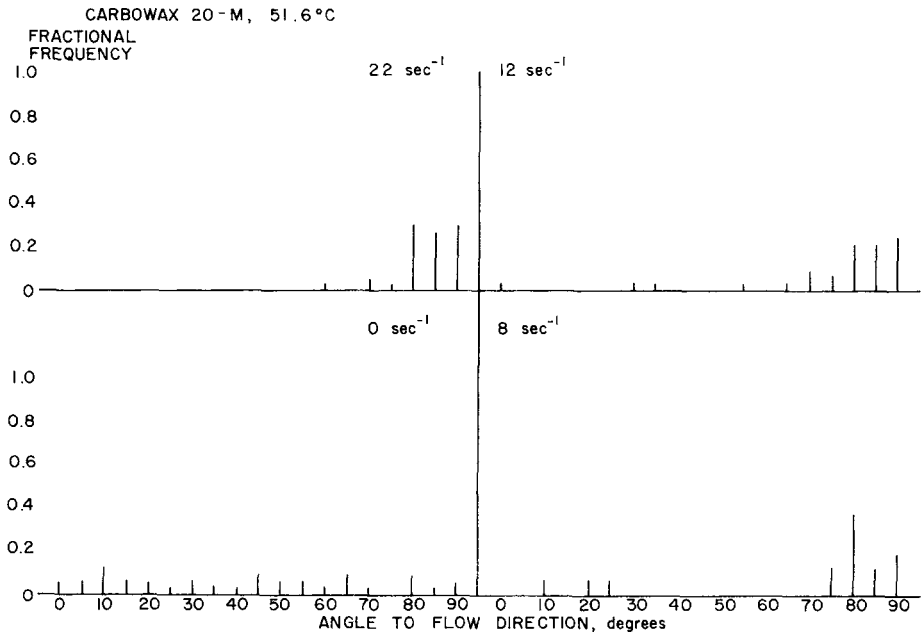

Fig. 5. Angular distribution of long axes of rod-like crystalline aggregates to the flow direction for Carbowax 20-M at 51.6°C for various shear rates.

out at 12 sec^{-1}. Separate crystallization runs were conducted with the polarizer set at 0°, 45°, and 90° to the flow direction for both H_v- and V_v-type scattering.

Light scattering occurs because of density fluctuations and/or anisotropy of the polarizability of the scattering medium. Resolution of these contributions may be obtained through appropriate analysis of the H_v- and V_v-type scattering patterns.[36] The V_v pattern for the quiescent case possesses a symmetric circular pattern typical of crystallizing polymer melts. Additionally, the pattern is of a grainy texture, indicating a small number of scattering entities. This is to be expected from the low nucleation density observed in the material under consideration. Because the particles are quite large relative to the wavelength of the light (0.632 μ), there is a rapid angular decrease in scattering intensity for all scattering cases.

The V_v-type patterns for the sheared cases show an elongation parallel to the flow direction. As has been shown by Stein and Rhodes[29] and Gieniewski and Moore,[37] the elongation of the scattering pattern will be perpendicular to the long axis of the scattering entity. Hence, the scattering entities are rod-like and oriented preferentially perpendicular to the flow direction. V_v scattering patterns with the polars set parallel to the flow direction show an initial decrease in intensity with scattering angle and then a maxima. Measurement of the angular position of the maxima provides an indication of the size of the scattering entity through use of the relation

$$\frac{4\pi r}{\lambda} \sin\left(\frac{\theta}{2}\right) = 4.0$$

where λ is the wavelength of the light, θ is the angular position of the intensity maxima, and r is the radius of the scattering entity. This equation was originally derived for H_v scattering from spherulites. However, calculation of r at various crystallization times yields values in accord with sizes measured using polarized light microscopy.

The shape of the angularly dependent V_v intensity distributions is reminiscent of those seen by Picot, Stein, Motegi, and Kawai[38] in sheaf-like scattering entities. Hence, the rod-like entities seen in the polarizing microscope actually may be sheaf-like structures. Evidence that these are indeed lamellar sheaf-like structures is provided by the V_v scattering at 45° to the flow direction and the H_H scattering. These also show the elongation parallel to the flow direction but are much less intense than the V_v patterns. This indicates that the principal polarizability of rod-like entities is preferentially parallel to the flow direction. Taking this in conjunction with the angularly dependent intensity distribution of the V_v patterns suggests chain-folded lamellar sheaf-like scattering entities the long axes of which are oriented perpendicular to the flow direction.

The H_v-type patterns reinforce those conclusions drawn from the V_v-type patterns. The H_v (45°) patterns (taken with the polarizer set 45° to the flow direction) are the most intense and again show an elongation in the flow direction. The H_v and V_H patterns (analyzer perpendicular and parallel, respectively) are much less intense (at least 50 times) than those for the H_v (45°). H_v patterns taken for the quiescent case show almost no scattering intensity. This again indicates rod-like scattering entities with their principal

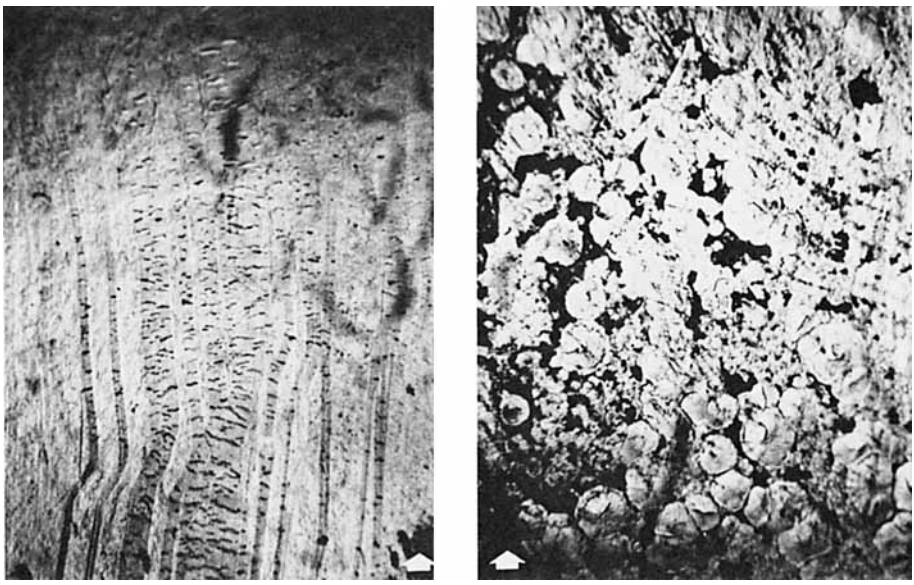

(a) (b)

Fig. 6. Epiphotomicrographs of Carbowax 20-M crystallized at 51.6°C under shear rate of 32 sec^{-1}: (a) row-like structures; (b) spherical crystalline aggregates

polarizabilities along the semiminor axes. These rods orient preferentially perpendicular to flow direction during shear and orient randomly under quiescent conditions.

These results are in accord with those made with the polarizing light microscope and are similar to those of Baranov, Volkov, Farshyan and Frenkel[39] on drawn melts of crystallizing polypropylene.

Epimicroscopy was used to study the surfaces of the sheared and unsheared samples after they had been completely crystallized and removed from the shearing device. All samples were shadowed with platinum to enhance the morphology.

Samples crystallized under quiescent conditions in the shearing device show radially symmetric crystalline arrays truncated by impingement. This is typical for a spherulitic morphology.

One of the typical morphologies observed in sheared samples consists of radially symmetric crystalline arrays; however, they are smaller than those formed in similar quiescent cases. Also, there is quite a bit of debris composed of even smaller crystalline aggregates. This is shown in Figure 6b.

Figure 6a shows the other morphology typical of the sheared material. This particular photograph is for a sample crystallized at 32 sec^{-1} and 51.6°C. There appear to be row-like structures with cross-striations lying perpendicular to the shear direction. The photograph in Figure 7 was taken by polarized light microscopy of a melt crystallizing under shear. The region of focus is near the bottom glass plate. Notice the row-like structures forming here. In this investigation, these row-like structures have never been observed to form within the melt, only near or on the surfaces of the glass shearing plates. They have never been observed to form under quiescent condi-

Fig. 7. Polarized light photomicrograph of row structure developing on bottom glass shearing plate during shear crystallization of Carbowax 20-M; 19.2 μ per scale division (arrow indicates flow direction).

tions. It is believed they form along fine scratches or heterogeneities on the glass plates. These results are quite simlar to those of Haas and Maxwell[24] for polybutene-1.

No studies were carried out on fracture surfaces of the samples, as they proved too irregular to be useful.

Carbon–platinum replicas of the fracture surfaces of samples crystallized under quiescent conditions show the large lamellar structures typical of bulk crystallized PEO.

Figure 8 is a replica of the fracture surface of material crystallized at

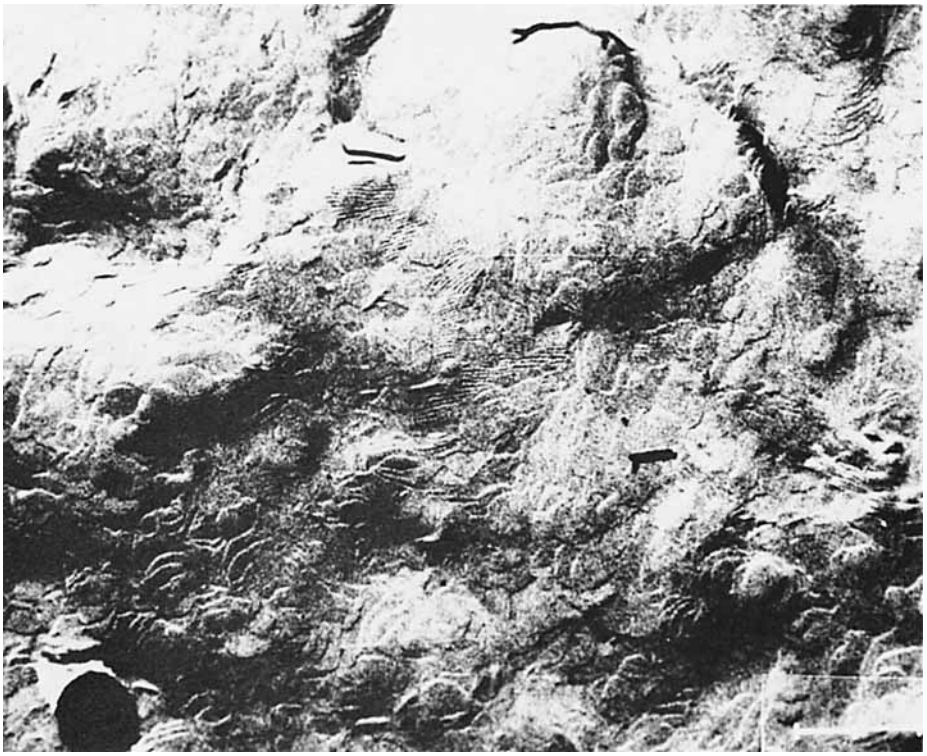

Fig. 8. Transmission electron micrograph of fracture surface of Carbowax 20-M crystallized at 32 sec^{-1} at 51.6°C.

51.6°C and 32 sec^{-1} shear rate. The long-range order present in the samples crystallized under quiescent conditions is absent.

Figure 9 is a replica of the surface of a sheared sample that was in contact with the bottom glass plate during the crystallization experiment. It was sheared at 32 sec^{-1} at 51.6°C. The row-like structure comes from areas that show similar structures on a larger scale in the epiphotographs. The shear direction runs diagonally from upper left to lower right. The lamellar structure perpendicular to the shear direction is quite evident and persists over distances on the order of 100 μ. These structures are reminiscent of those seen by Andrews[3] in stress-crystallized samples of natural rubber.

Wide-angle x-ray diffraction photographs of material crystallized under quiescent conditions at 51.6°C and material crystallized under a shear rate of 32 sec^{-1} at the same temperature were made. The material crystallized under quiescent conditions showed a typical ring pattern with a mottling of the rings similar to that seen in powder photographs when the sample has not been ground finely enough.

The shear crystallized sample showed an equatorial line broadening typical of oriented crystalline material. The mottled appearance of the diffraction rings has also disappeared. This would seem to indicate a finer morphology than is present in the unsheared sample.

DSC analysis showed no significant differences between the sheared and unsheared samples.

Fig. 9. Transmission electron micrograph of surface of Carbowax 20-M crystallized at shear rate of 32 sec^{-1} at 51.6°C; from the same region as Fig. 6a (arrow indicates flow direction).

DISCUSSION

Particle Orientation

The alignment of the crystallizing rod-like entities, with respect to the shear field produced in the apparatus, may be analyzed through the treatments of Jeffery[40] and Goldsmith and Mason.[41] The coordinate system and flow field to be considered are shown in Figure 10. Observation of the particle motions is made along the X_2 axis in the shearing apparatus used for this research. Translational motion is along the X_3 axis. It has been previously shown that the rod-like entities are in the form of prolate ellipsoids. Let b_1 and b_2 be the semimajor and semiminor axes, respectively, of these prolate ellipsoids. It has been shown by Jeffery that the angular rotation for the axis of revolution is given by

$$\dot{\phi}_1 = \frac{\dot{\gamma}}{a^2 + 1}(a^2 \cos^2 \phi_1 + \sin^2 \phi_1) \tag{1}$$

while the angular rotation of the b_1 axis is given by

$$\dot{\theta}_1 = \frac{\dot{\gamma}(a^2 - 1)}{4(a^2 + 1)}(\sin 2\phi_1 \sin 2\theta_1) \tag{2}$$

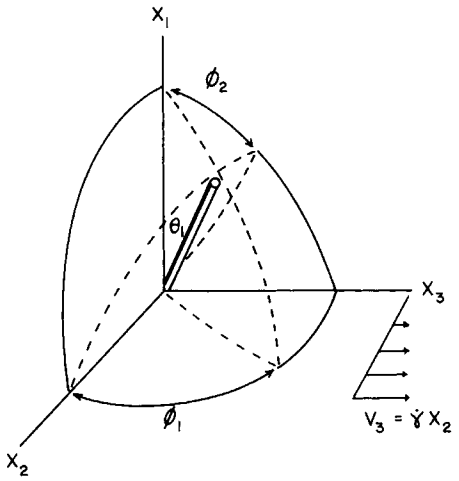

Fig. 10. Flow field coordinate system.

where a is the aspect ratio b_1/b_2 and $\dot{\gamma}$ is the shear rate. Likewise, the spin about the axis of symmetry (the b_1 axis) is given by

$$w = \frac{1}{2}(\dot{\gamma} \cos \theta_1). \tag{3}$$

The motion of the axis of revolution of the prolate ellipsoid is described by

$$\tan \phi_1 = a \tan \left(\frac{\dot{\gamma} t}{a + 1/a}\right) = a \tan \left(\frac{2\pi t}{P}\right) \tag{4}$$

which is obtained by integration of eq. (1). Here, t is an arbitrary time during the observation of the particle motion, and P is the period of rotation, which is given by

$$P = \frac{2\pi}{\dot{\gamma}}(a + 1/a). \tag{5}$$

Therefore, $\dot{\phi}_1$ will have maxima at ϕ_1 values of 0 and π and minima at ϕ_1 values of $\pi/2$ and $3\pi/2$.

The motion of the ends of the prolate ellipsoids may be had from eqs. (1) and (2) and is given by

$$\tan \theta_1 = \frac{Ca}{(a^2 \cos^2 \phi_1 + \sin^2 \phi_1)^{1/2}} \tag{6}$$

where C is a constant of integration defined as the orbit constant. This motion corresponds to the ends of spheroids generating a pair of symmetrical ellipses. The eccentricity of these ellipses is given by C, while the principal axes are given by $\tan^{-1}(Ca)$ at the maximum and minimum values of $\dot{\phi}_1$, $\phi_1 = 0, \pi$ and $\phi_1 = \pi/2, 3\pi/2$.

The value of C may vary from zero to infinity. When $C = 0$, θ_1 will be

equal to zero at all values of ϕ_1. This corresponds to a continuous spin of the axis of revolution about X_1 at a rate of $w = \dot{\gamma}/2$ as given by eq. (3). If C is equal to infinity, θ_1 will equal $\pi/2$ at all values of ϕ_1, $\dot{\phi}_1$ will be variable, and there will be no axial spin. It has been shown by several investigators[42–47] that the motions predicted by these equations are observed experimentally.

Jeffery has shown theoretically that the motion of the prolate ellipsoids will be such that energy dissipation tends to be a minimum. This corresponds to $C = 0$. It has been experimentally observed[48] that at low Reynolds numbers in Newtonian fluids where there are no particle interactions or sedimentation, motion of the rod-like particles will indeed correspond to $C = 0$ and not change with time. The same behavior is observed in viscoelastic materials. Hence, the prolate ellipsoids will align their major axes along the X_1 direction and spin about their axes of revolution at a rate of $w = \dot{\gamma}/2$.

The motion of the prolate ellipsoids, as viewed along the X_2 axis (direction of observation for this research) can be described as a rocking motion, the limits of which are the projections, on the X_1X_3 plane, of the major axes of the symmetric ellipses generated by the ends of the prolate ellipsoids. As previously shown, these are given by $\tan^{-1}(Ca)$. Since $C = 0$ for the case being considered, ϕ_2, the angle through which the particle rocks, will also be zero. Hence, the motion of the rod-like particles will correspond to a translation along the flow direction with the long axes of the rods aligned, on the average, parallel to the X_1 axis, i.e., perpendicular to the flow direction. The particles will also spin about their long axes at a rate $w = \dot{\gamma}/2$. Observations in the system being considered correspond to this description. The ellipsoids can be seen to spin about their long axes, though it has not been possible to measure this rate.

It should also be pointed out that in non-Newtonian fluids[49,50] and in Newtonian fluids at high Reynolds numbers,[51,52] the value of C will change with time and assume those values which correspond to maximum energy dissipation.

In this research, the rod-like nature of the developing crystallites is not unique to the shear crystallized material. Indeed, Bernauer[53] postulated in 1929 that spherulites began as lamellar rod-like entities the ends of which splayed to give sheaf-like structures which, in turn, grew into spherulites. This growth process has been observed and described by Morse and Donnay[54] for inorganic materials and by Adams and Stein[55] for polymeric materials. This mechanism seems to be that generally observed for the early stages of spherulite growth regardless of the material. If the nucleation density is sufficiently high, such as in cellulose, the morphology never develops past that of the rod-like structure.

Let it be assumed that the initial rod-like or sheaf-like structures are composed of stacked lamellae or dendrites which are, in turn, made up of folded polymer chains. The chains will therefore be preferentially aligned perpendicular to the long axis of the rod. If, in turn, the rods were in a shear field such as that previously described, the chains would lie in a series of planes parallel to the X_2X_3 plane and perpendicular to the X_1 axis. Assuming the material being crystallized possessed a high nucleation density, it would be possible for the morphology never to develop past the rod-like stage. The rods would orient perpendicularly to the flow direction, impinge and lock the

orientation into the completely crystallized mass. This would produce a final morphology, except for the nucleation lines, that would be difficult to discern from the twisted lamellar structure proposed by Hill and Keller[18] for material crystallized under low stress.

As shown by polarizing microscopy and light-scattering studies, carried out under identical crystallization times and conditions, the initial morphology of the crystallizing PEO is rod-like or, perhaps more accurately, sheaf-like. The fact that the principal polarizability of the sheaf-like entities lies perpendicular to the long axis of the rods and, hence, parallel to the flow direction, would indicate a preferential alignment of the molecular chains in planes parallel to the flow direction and perpendicular to the X_1 axis of the flow field. This behavior, with the exception that the PEO possesses a low nucleation density under the conditions studied, relates favorably to the comparison made with the postulated structures of Hill and Keller.

That this does not occur in the final morphology for the conditions studied is demonstrated by the fact that under shear the material is seen to develop ultimately into nearly spherical entities. Further, the row-like structures demanded by the models of Hill and Keller have not been observed, in this research, to form within the melt. Row-like structures have been shown to form on the glass plate surfaces by polarized light and electron microscopy. It is felt that these structures form on surface heterogeneities, perhaps due to higher stresses generated by chains absorbed on the heterogeneities.

It has not been possible to microscopically determine a change in the optical anisotropy of the single particles in going from the quiescent to the sheared systems. Light scattering has thus far been unable to determine if there is an orientational change within each particle, as it is an averaging technique and the particles are randomly oriented under quiescent conditions. Hence, it has not been experimentally established that there is any orientational change within each particle when it is subjected to a shear field during its crystallization.

Baranov et al.[39] have used light-scattering techniques to study the behavior of polyethylene and polypropylene fibers as they crystallize upon being spun from the melt. It was observed that ellipsoidal spherulites were formed within the fibers with their long axes perpendicular to the stretch direction. The aspect ratio of the ellipsoids increased as the stretching was increased. Orientation of the crystallizing material was shown by x-ray diffraction patterns of the material after it had completely crystallized. The authors postulated that because of the tangential orientation of the chains in spherulites of the materials studied, it would take extra work to grow lamellae in directions along that of the stretching, or flow, and less work to grow lamellae in directions perpendicular to the stretch, or flow. Hence, the spherulites grow in the forms of ellipsoids, the long axes (fastest lamellar growth direction) of which are perpendicular to the stretch direction. Whether these processes are at work in the PEO system studied has not been determined. It will be recalled that the x-ray diffraction patterns showed very little orientation of the shear crystallized PEO. Also, the rod-like entities in the sheared PEO eventually grow into nearly spherical entities which do not appear to be true spherulites, but rather less ordered spherical crystalline aggregates. Therefore, it would appear that the processes postulated by Baranov et al. do not

contribute greatly to the gross morphology of the rod-like structures, but may affect the internal order of the particles.

Crystalline Texture

It appears that shear crystallization affects the texture of the resulting crystalline entities on a level below that of the orientation of the rod-like structures. Consideration of the electron micrographs of the fracture surfaces of the sheared and unsheared samples demonstrates a definite difference in the lamellar texture. The unsheared samples possess large flat lamellae which run over long distances. This is in contrast to the fracture surfaces of the sheared material which show a finer lamellar morphology.

Careful examination of the wide-angle x-ray diffraction patterns of already crystallized samples shows a mottled appearance in the rings of the quiescently crystallized material. This mottling is quite similar to that seen in powder diffraction rings when the powder has not been ground to a fine enough texture. This would indicate that the quiescent sample possessed rather large scattering entities. On the other hand, the sheared sample showed no mottling of the diffraction rings. This would seem to be further evidence that the texture of the sheared material was finer than that of the unsheared material.

The finer structure of the sheared material may be due to two effects. The first of these is fracture of preexisting crystalline aggregates during shear. It is rather apparent from comparisons of the epimicrographs of the sample surfaces that the sheared material still possesses the radially symmetric crystalline aggregates seen in the unsheared material. However, these aggregates appear smaller in the sheared material, are spaced farther apart, and are interspersed with what appears to be crystalline debris.

Further evidence for fracture during flow has been shown by Fritzsche[35] and will be given in a paper dealing with the kinetics of the system.

Sheldon[56] has studied the effect of extrusion rate and temperature on the crystallization of PET. It was found that as the melt temperature was lowered, increasing the extrusion rate decreased the rate of sample crystallization. This was ascribed to the possibility of the shear stresses disrupting very small or just formed nuclei. It would seem reasonable that similar processes may be occurring in the PEO system being studied here. The stresses generated within the shear field disrupt small or just formed nuclei and return them to the melt or amorphous state. However, those particles which survive past a certain critical size grow faster (perhaps due to mechanisms similar to those suggested by Baranov et al.) and, hence, there are a smaller number of crystalline aggregates for a given fraction of transformed material for the sheared case than the unsheared case.

Further, it is believed that particle fracture has been observed visually using polarized light microscopy during crystallization of the material. However, the system is constantly moving and it is quite difficult to unequivocally determine that the fracture process is indeed occurring. Attempts have been made to produce motion pictures of the process so that it could be studied at slower speeds. Unfortunately, the combinations of filming speed and illumination intensity available have not proved sufficient for a detailed analysis to be conducted.

Evidence presented thus far is necessary, but not sufficient, to support the hypothesis of particle fracture as a major contributor to the morphology and kinetics of the sheared systems. Qualitative data tend to indicate that fracture is indeed occurring. However, from this research, there is not sufficient quantitative evidence to discern between fracture and increased nucleation.

One factor which may negate the postulated fracture process is the appearance of the electron micrographs of the fracture surfaces of the sheared material. While it is true that the overall lamellar texture is finer than that of the unsheared material, it would be expected that crystalline debris generated by the fracturing process should be present.

In all probability, both fracture and increased nucleation rate are active in determining the morphology and kinetics of the sheared samples. The fracture of the PEO studied is not difficult to conceive when it is considered that on a macroscale the material is similar to paraffin wax in its strength. Evidence for increased primary and secondary nucleation will be discussed in a later paper.

This work was supported in part by Grant No. GH 34453X from the National Science Foundation.

References

1. L. R. G. Treloar, *Trans. Faraday Soc.*, **37,** 84 (1941).
2. A. N. Gent, *Trans. Faraday Soc.*, **50,** 521 (1954).
3. E. H. Andrews, *Proc. Roy. Soc.*, **A271,** 562 (1964).
4. T. Kawai, M. Iguchi, and H. Tonami, *Kolloid-Z.*, **221,** 28 (1967).
5. A. Keller, *Kolloid-Z.*, **165,** 15 (1959).
6. D. A. Blackladder and H. M. Scleinitz, *Nature*, **200,** 778 (1963).
7. A. J. Pennings and A. M. Kiel, *Kolloid-Z.*, **205,** 160 (1965).
8. P. H. Lindenmeyer, *S.P.E. Trans.*, **4,** 1 (1964).
9. A. J. Pennings, J. M. A. A. Van der Mark, and H. C. Booij, *Kolloid-Z.*, **236,** 99 (1970).
10. A. J. McHugh and J. M. Schultz, Paper AL3, American Physical Society Meeting, Division of High Polymer Physics, Atlantic City, N.J., March, 1972.
11. F. M. Willwonth, A. Keller, I. M. Ward, and T. Williams, *J. Poly. Sci. A2,* **6,** 1627 (1967).
12. A. Keller and M. J. Machin, *J. Macromol. Sci. B,* **1,** 41 (1967).
13. A. Keller and M. J. Machin, in *Polymer Systems: Deformation and Flow,* Macmillan, London, 1967, p. 97.
14. B. Wunderlich, C. M. Cormier, A. Keller, and M. J. Machin, *J. Macromol. Sci. B,* **1,** 93 (1967).
15. G. E. Ashby, Preprint 27B, Symposium on Effects of Molecular Orientation on Structure and Properties of Polymers, Part I, Pittsburgh, Pa., May 7–10, 1964, sponsored by A.I.Ch.E.
16. A. K. Van der Vegt and P. P. A. Smit, Paper No. 17, Symposium on Advances in Polymer Science and Technology, London, May 3–5, 1966, sponsored by the Society of Chemical Industry.
17. A. Keller and M. J. Machin, *J. Macromol. Sci. B,* **1,** 41 (1967).
18. M. J. Hill and A. Keller, *J. Macromol. Sci. B3,* **1,** 153 (1969).
19. R. B. Williamson and W. F. Busse, *J. Appl. Phys.*, **38,** 4187 (1967).
20. H. D. Keith, F. J. Padden, and R. G. Vadimsky, *J. Polym. Sci. A,* **4,** 267 (1966).
21. H. D. Keith, F. J. Padden, and R. G. Vadimsky, *J. Appl. Phys.*, **37,** 4027 (1966).
22. K. Kobayashi and T. Nagasawa, *How Sheared Melts of Polymers Behave in the Crystallization Process,* Institute for Chemical Research, Kyoto University, 1968.
23. T. Kawai, R. Kamoto, K. Ehara, T. Matsumoto, and H. Maeda, *Sen-I Gakkaishi,* **26,** 80 (1970).
24. T. W. Haas and B. Maxwell, *Polym. Sci. Eng.*, **9,** 225 (1969).
25. P. H. Geil, *Polymer Single Crystals,* Interscience, New York, 1963, Chap. 2.

26. P. H. Geil, in *Growth and Perfection of Crystals,* R. H. Doremus, B. W. Roberts, and D. Turnbull, Eds., Wiley, New York, 1958.
27. H. Staudinger and R. Signer, *Z. Krist.*, **70,** 193 (1929).
28. F. P. Price and R. W. Kilb, *J. Polym. Sci.*, **57,** 395 (1962).
29. R. S. Stein and M. B. Rhodes, *J. Appl. Phys.*, **31,** 1873 (1960).
30. H. Tadokoro, Y. Chatani, T. Yoshihara, S. Tahora, and S. Murahashi, *Makromol. Chem.*, **73,** 109 (1964).
31. L. Mandelkern, *Chem. Rev.*, **56,** 903 (1956).
32. W. J. Barnes, W. G. Leutzel, and F. P. Price, *J. Phys. Chem.*, **65,** 1742 (1961).
33. W. Banks and A. Sharples, *Makromol. Chem.*, **67,** 42 (1963).
34. P. Erhardt and R. S. Stein, *J. Polym. Sci. B,* **3,** 553 (1965).
35. A. K. Fritzsche, Doctoral Dissertation, University of Massachusetts, November 1972.
36. R. S. Stein, in *Newer Methods of Polymer Characterization,* B. Ke, Ed., Interscience, New York, 1964.
37. C. Gieniewski and R. S. Moore, *Macromol.*, **2,** 385 (1969).
38. C. Picot, R. S. Stein, M. Motegi, and H. Kawai, *J. Polym. Sci. A2,* **8,** 2115 (1970).
39. V. G. Baranov, T. I. Volkov, G. S. Farshyan, and S. Ya. Frenkel, *J. Polym. Sci. C,* **30,** 305 (1970).
40. G. B. Jeffery, *Proc. Roy. Soc.* (London), **A102,** 161 (1922).
41. H. L. Goldsmith and S. G. Mason, *The Microrheology of Dispersions,* Technical Report No. 437, Pulp and Paper Research Institute of Canada.
42. C. E. Chaffey and S. G. Mason, *J. Colloid Sci.*, **19,** 525 (1964).
43. B. J. Trevelyan and S. G. Mason, *J. Colloid Sci.*, **6,** 354 (1951).
44. W. Bartok and S. G. Mason, *J. Colloid Sci.*, **12,** 243 (1957).
45. R. St. J. Manley and S. G. Mason, *J. Colloid Sci.*, **7,** 354 (1952).
46. O. L. Forgacs and S. G. Mason, *J. Colloid Sci.*, **14,** 457 (1959).
47. H. L. Goldsmith and S. G. Mason, *J. Fluid Mech.*, **12,** 88 (1962).
48. E. Anczurowski and S. G. Mason, *J. Colloid Interfac. Sci.*, **23,** 533 (1967).
49. P. G. Saffman, *J. Fluid Mech.*, **1,** 540 (1956).
50. G. I. Taylor, *Proc. Roy. Soc.* (London), **A103,** 58 (1923).
51. A. Karnis, H. L. Goldsmith, and S. G. Mason, *Nature,* **200,** 159 (1963).
52. A. Karnis, H. L. Goldsmith, and S. G. Mason, *J. Colloid Interfac. Sci.*, **22,** 531 (1966).
53. A. Sharples, *Introduction to Polymer Crystallization,* Arnold Press, London, 1966, p. 15.
54. H. W. Morse and J. D. H. Donnay, *Amer. Minerologist,* **21,** 391 (1936).
55. G. C. Adams and R. S. Stein, *J. Polym. Sci. A2,* **6,** 31 (1968).
56. R. P. Sheldon, *Polymer,* **4,** 213 (1963).

Received July 24, 1974
Revised July 2, 1975